JNeurosci
THE JOURNAL OF NEUROSCIENCE

Research Articles: Systems/Circuits

Regional delta waves in human rapid-eye movement sleep

Giulio Bernardi[1,2], Monica Betta[2], Emiliano Ricciardi[2], Pietro Pietrini[2], Giulio Tononi[3] and Francesca Siclari[1]

[1]*Center for Investigation and Research on Sleep, Lausanne University Hospital, Lausanne, Switzerland*
[2]*MoMiLab Research Unit, IMT School for Advanced Studies, Lucca, Italy*
[3]*Dept. of Psychiatry, University of Wisconsin, Madison, WI, USA*

https://doi.org/10.1523/JNEUROSCI.2298-18.2019

Received: 5 September 2018

Revised: 28 November 2018

Accepted: 4 January 2019

Published: 8 February 2019

Author contributions: G.B., E.R., P.P., G.T., and F.S. designed research; G.B. and F.S. performed research; G.B., M.B., and F.S. analyzed data; G.B., M.B., and F.S. wrote the first draft of the paper; G.B., M.B., E.R., P.P., G.T., and F.S. edited the paper; G.B. and F.S. wrote the paper.

Conflict of Interest: The authors declare no competing financial interests.

This work was supported by the Swiss National Science Foundation (Ambizione Grant PZ00P3_173955; F.S.), the Divesa Foundation Switzerland (F.S.), the Pierre-Mercier Foundation for Science (F.S.), the Bourse Pro-Femme of the University of Lausanne (F.S.), and a Research Support Grant of the University of Lausanne (F.S. and G.B.). The authors thank Brady Riedner, Michele Bellesi, Josh J. LaRoque and Xiaoqian Yu for technical assistance and help with data collection.

Correspondence: Francesca Siclari, MD, CHUV, Centre d'investigation et de recherche sur le sommeil, Rue du Bugnon 46, CH-1011, Lausanne, Switzerland, francesca.siclari@chuv.ch; Giulio Bernardi, MD, PhD, IMT School for Advanced Studies Lucca, Piazza S.Francesco, 19, IT-55100, Lucca, Italy, giulioberna@gmail.com

Cite as: J. Neurosci 2019; 10.1523/JNEUROSCI.2298-18.2019

Regional delta waves in human rapid-eye movement sleep

Giulio Bernardi [1,2,*], Monica Betta [2], Emiliano Ricciardi [2],
Pietro Pietrini [2], Giulio Tononi [3], Francesca Siclari [1,*]

[1] *Center for Investigation and Research on Sleep, Lausanne University Hospital, Lausanne, Switzerland*
[2] *MoMiLab Research Unit, IMT School for Advanced Studies, Lucca, Italy*
[3] *Dept. of Psychiatry, University of Wisconsin, Madison, WI, USA*

Abbreviated Title: *Delta EEG waves in REM-sleep*

Number of Pages:
Number of Figures: 10
Number of Tables: 1

Abstract: 225 words
Introduction: 649 words
Discussion: 1925 words

Correspondence (*):

Francesca Siclari, MD
CHUV, Centre d'investigation et de recherche sur le sommeil
Rue du Bugnon 46
CH-1011, Lausanne, Switzerland
francesca.siclari@chuv.ch

Giulio Bernardi, MD, PhD
IMT School for Advanced Studies Lucca
Piazza S.Francesco, 19
IT-55100, Lucca, Italy
giulioberna@gmail.com

Conflict of Interest
The authors declare no competing financial interests.

Acknowledgments
This work was supported by the Swiss National Science Foundation (Ambizione Grant PZ00P3_173955; F.S.), the Divesa Foundation Switzerland (F.S.), the Pierre-Mercier Foundation for Science (F.S.), the Bourse Pro-Femme of the University of Lausanne (F.S.), and a Research Support Grant of the University of Lausanne (F.S. and G.B.). The authors thank Brady Riedner, Michele Bellesi, Josh J. LaRoque and Xiaoqian Yu for technical assistance and help with data collection.

Abstract

Although the EEG slow wave of sleep is typically considered to be a hallmark of Non Rapid Eye Movement (NREM) sleep, recent work in mice has shown that slow waves can also occur in REM sleep. Here we investigated the presence and cortical distribution of negative delta (1-4 Hz) waves in human REM sleep by analyzing high-density EEG sleep recordings obtained in 28 healthy subjects. We identified two clusters of delta waves with distinctive properties: 1) a fronto-central cluster characterized by ~2.5-3.0 Hz, relatively large, notched *delta* waves (so-called 'sawtooth waves') that tended to occur in bursts, were associated with increased gamma activity and rapid eye movements, and upon source modeling, displayed an occipito-temporal and a fronto-central component; and 2) a medial-occipital cluster characterized by more isolated, slower (<2 Hz) and smaller waves that were not associated with rapid eye movements, displayed a negative correlation with gamma activity and were also found in NREM sleep. Thus, delta waves are an integral part of REM sleep in humans, and the two identified subtypes (sawtooth and medial-occipital slow waves) may reflect distinct generation mechanisms and functional roles. Sawtooth waves, which are exclusive to REM sleep, share many characteristics with ponto-geniculo-occipital (PGO) waves described in animals and may represent the human equivalent or a closely related event while medial-occipital slow waves appear similar to NREM sleep slow waves.

Key words: REM sleep, hd-EEG, sawtooth wave, slow wave, PGO wave.

Significance Statement

The EEG slow wave is typically considered a hallmark of NREM sleep, but recent work in mice has shown that it can also occur in REM sleep. By analyzing hd-EEG recordings collected in healthy adult individuals, we show that REM-sleep is characterized by prominent delta waves also in humans. In particular, we identified two distinctive clusters of delta waves with different properties: a fronto-central cluster characterized by faster, activating 'sawtooth waves' that share many characteristics with PGO waves described in animals, and a medial-occipital cluster containing slow waves which are more similar to NREM-sleep slow waves. These findings indicate that REM-sleep is a spatially and temporally heterogeneous state, and may contribute to explain its known functional and phenomenological properties.

Introduction

Sleep is characterized by relative quiescence and reduced responsiveness to external stimuli. Based on electrophysiological hallmarks, sleep is divided into non-rapid eye movement (NREM-)sleep and REM-sleep. While REM-sleep is characterized by rapid eye movements and muscular atonia, and by a tonically 'activated' (low voltage, high frequency) EEG resembling that of wakefulness (Aserinsky and Kleitman, 1953; Dement and Kleitman, 1957), hallmarks of NREM-sleep include high-amplitude, slow waves (≤4 Hz) and spindles (12-16 Hz) (Steriade et al., 1993, 2001). Given these differences, it has been commonly assumed that wakefulness, NREM-sleep and REM-sleep represent mutually exclusive 'global' states. This view has been recently challenged by a growing body of evidence indicating that many features of sleep are essentially local, and that islands of sleep- and wake-like activity may coexist in different brain areas (Siclari and Tononi, 2017).

EEG slow waves of NREM-sleep occur when neurons become *bistable* and oscillate between two states: a hyperpolarized *down-state* characterized by neuronal silence (*off-period*), and a depolarized *up-state* during which neurons fire (*on-period*) (Steriade et al., 2001). Intracranial recordings in humans have shown that during stable NREM-sleep, slow waves can be restricted to some localized areas and occur out of phase with other cortical regions (Nir et al., 2011). The regional distribution of slow wave activity (SWA) has been shown to be modulated by recent experience and learning (e.g., (Huber et al., 2004, 2006)). Local slow waves, involving small portions of the cortical mantle, have also been shown to occur in awake humans (Hung et al., 2013; Bernardi et al., 2015) and rodents (Vyazovskiy et al., 2011, 2014), particularly in conditions of sleep deprivation. Importantly for the purpose of our study, recent work demonstrated that in mice (Funk et al., 2016), slow waves with neuronal *off-periods* may also occur during REM-sleep in primary visual (V1), sensory (S1) and motor (M1) areas, mainly in cortical layer 4. By contrast, associative areas, such as V2, S2, or the retrosplenial cortex, showed the typical activated pattern of REM-sleep. It is currently unknown whether similar regional differences and local slow waves also exist in human REM-sleep. In fact, while great effort has been dedicated to the study of prominent features of REM-sleep, such as theta (5-8 Hz) or high-frequency (>25 Hz) activity, little attention has been given to delta (≤4 Hz) waves during this sleep stage. A few studies found that *delta* power (1-4 Hz) in REM-sleep had a different topographic distribution with respect to NREM-sleep (Tinguely et al., 2006; Ferrara and De Gennaro, 2011). In addition, we recently showed that both in REM and NREM sleep, reduced *delta* power in posterior cortical regions is associated with dreaming (Siclari et al., 2017), suggesting a similar functional significance of slow waves across states. By analyzing slow wave characteristics in NREM sleep, we identified two types of slow waves with distinct features: large, steep fronto-central type I slow waves, which are likely generated in a bottom-up manner by arousal systems, and smaller type II slow waves, which are diffusely distributed over the cortical mantel and probably underlie a cortico-cortical synchronization mechanism (Siclari et al., 2014). Further analyses showed that the two types of slow waves are differentially related to dreaming (Siclari et al., 2018).

In the present study we aimed at investigating the presence and cortical distribution of delta (1-4 Hz) waves in human REM-sleep using high-density EEG recordings, which provide an excellent combination of temporal and spatial resolution. We also wanted to determine whether we could identify different delta wave types with

distinct characteristics, similarly to NREM sleep. Sawtooth waves of REM-sleep, for instance, are known to peak in the *delta* range (~3 Hz), but their properties and cortical distributions have not been systematically investigated in humans using techniques with a high spatial resolution. Therefore, we expected to identify at least two types of delta waves in human REM-sleep, corresponding to sawtooth waves and local slow waves involving primary sensory cortices.

Material and Methods

Participants. Overnight high-density (hd-)EEG recordings (Electrical Geodesics, 256 electrodes, 500 Hz sampling frequency) were obtained in 16 healthy volunteers (age 24.9±4.5, 8 females; 13 right-handed). NREM-sleep data (but not REM-sleep data) from 10 of these subjects has been reported in a previous publication (Bernardi et al., 2018). All participants had a sleep duration of ~7 h/night, consistent bed/rise times, no daytime nap habits and no excessive daytime sleepiness (total scores in the Epworth Sleepiness Scale ≤10; (Johns, 1991)). A clinical interview was performed to exclude a history of sleep, medical and psychiatric disorders. The study was approved by the IRB of University of Wisconsin-Madison. Each participant signed an IRB-approved informed consent form before enrollment into the study.

Since wake data was not available from the above subjects, specific analyses aimed at comparing sleep- and wake-related brain activity (see below) were performed in a different sample of 12 healthy adult individuals (age 25.5 ± 3.7, 6 females) who underwent overnight hd-EEG sleep recordings after having spent 8 h in the sleep laboratory while watching movies (analyses of wake and NREM-sleep data from these subjects has been reported in (Bernardi et al., submitted)). These recordings were performed at Lausanne University Hospital, under a research protocol approved by the local ethical committee.

EEG data preprocessing. All hd-EEG recordings (Madison dataset) were first-order high-pass filtered at 0.1 Hz and band-pass filtered between 0.5 and 58 Hz. For scoring purposes, four of the 256 electrodes -two placed at the outer canthi of the eyes, and two placed above and below one of the two eyes- were used to monitor eye movements (electrooculography, EOG), while electrodes located in the chin-cheek region were used to evaluate muscular activity (electromyography, EMG). Sleep scoring (Table 1) was performed over 30s epochs according to standard criteria by a sleep medicine board certified physician (Iber et al., 2007). All the epochs scored as REM-sleep were identified and extracted.

[Table 1]

Detection and classification of delta waves. For each subject and recording, channels containing artifactual activity were visually identified, rejected, and replaced with data interpolated from nearby channels using spherical splines (NetStation, Electrical Geodesics Inc.). Potential ocular, muscular and electrocardiograph artifacts were removed using Independent Component Analysis (ICA) in EEGLAB (Delorme and Makeig, 2004). An algorithm based on the analysis of consecutive signal zero-crossings (Riedner et al., 2007) was adapted for the detection of delta waves in REM-sleep. Before application of the algorithm, the signal of each channel was referenced to the average of the two mastoid electrodes, down-sampled to 128 Hz, and filtered

between 1 and 10 Hz (the upper limit of the filter was selected to minimize wave shape and amplitude distortions). For each detected half-wave with duration between 125 and 500 ms (1-4 Hz), the following properties were extracted and stored for further analyses: negative amplitude (μV), duration (ms) and number of negative peaks (np/w). As described in previous work (Riedner et al., 2007), the negative peaks were identified based on the zero crossings of the EEG signal derivative corresponding to the negative half-wave, after application of a 50-ms moving-average filter. The density of slow waves (waves per minute; w/min) was also computed.

Preliminary analyses revealed two spatially distinct clusters of low-frequency waves in the 1-4 Hz range: a fronto-central and a medial-occipital cluster characterized by different frequencies and amplitudes (Figure 1). For this reason, subsequent analyses were in part adapted to the characteristics of the two delta wave types (see Results).

Temporal clusterization of delta waves. We investigated the tendency of delta waves to occur in bursts. Bursts were defined as a series of at least 3 consecutive waves whose maximum negative peaks were less than 750 ms apart. For this analysis a slightly broader half-wave duration limit (range 1-5 Hz) was used to minimize exclusion of potential 'borderline' delta waves within a burst. An amplitude constraint was applied so that the amplitude of each consecutive wave in the burst had to vary by less than 25% (relative to the preceding wave). No other amplitude or duration threshold was applied.

Relationship with rapid eye movements. Individual rapid eye movements (EMs) were identified using an automatic detection algorithm (Betta et al., 2013, 2015). In brief, the algorithm detects local peaks in the sum of the Haar Wavelet Transform coefficients in a specific frequency range (0.8-5 Hz) to determine the exact timing and duration of each eye movement (Betta et al., 2013). Bursts of rapid EMs were defined as serial EMs (2 or more) separated by less than 1 s. *Isolated* rapid EMs/bursts were defined as single EMs/bursts preceded and followed by periods of at least 5s without rapid EMs. To determine how delta waves relate to rapid EMs, for each isolated EM, wave density was calculated in two windows corresponding to 1 s before the onset of the first EM ('pre') and 1 s after the end of the last EM ('post').

Phasic REM periods were defined as time periods longer than 5 s that were occupied by EMs for more than 50% of their length. EMs in this time window had to be less than 2s apart to be considered as part of the same phasic period. Tonic REM episodes were defined as time periods longer than 5s that were completely free from any EMs. The average density of fronto-central and medial-occipital waves was calculated in all phasic and tonic periods.

In order to increase the signal-to-noise ratio of these analyses, amplitude thresholds corresponding to 10 μV and 3 μV were applied for fronto-central and medial-occipital delta waves, respectively.

Relationship with high-frequency activity. Next, in light of previous observations linking NREM slow waves to changes in high-frequency EEG activity (Valderrama et al., 2012; Siclari et al., 2014), we examined the temporal relation between *gamma* and *delta* power during delta waves of REM-sleep. For each wave, the band-specific instantaneous signal power was computed as the root mean square (RMS, time-window = 40 ms, step = 20 ms) of the *delta* (0.5-4 Hz) and *gamma* band-pass filtered (30-55 Hz) signals in a 2 s time-window centered on the negative peak of the delta wave. To increase the signal-to-noise ratio, amplitude thresholds corresponding to 10

μV and 3 μV were applied for fronto-central and medial-occipital delta waves, respectively. For each subject, *delta* and *gamma* RMS time-series were z-score transformed in a 600 ms time window centered on the wave negative peak, and then averaged across all the detected waves.

Overnight changes in delta waves. Slow waves of NREM-sleep are known to change in density and amplitude across a night of sleep (Riedner et al., 2007; Bernardi et al., 2018). Thus, here we evaluated whether delta waves of REM-sleep undergo similar changes. Specifically, for each subject, we first calculated the mean density and amplitude of delta waves within each REM-sleep cycle. Then, the magnitude of the density/amplitude changes ('slope') was calculated across cycles using least square linear regression (considering as independent variable the absolute sleep time at half of the corresponding REM-sleep cycle).

Relationship with delta waves of NREM-sleep. In order to evaluate similarities and differences between delta waves of REM- and NREM-sleep, additional analyses were performed on a sub-sample of 10 subjects (4 females, age 25.4±4.7). NREM data of these 10 subjects was preprocessed using the same procedures described above as part of a previous publication aimed at exploring different types of slow waves during NREM-sleep (Bernardi et al., 2018). For these subjects, the same negative half-wave detection algorithm described above was applied to N2 and N3 sleep data of the whole night on a channel-by-channel basis. Then, half-waves with duration 125-250 ms (>2 Hz) and 300-500 ms (<2 Hz) were identified to calculate mean density (w/min) and negative amplitude (μV). A non-parametric Friedman test was applied to investigate potential stage-dependent (N2/N3/REM) differences in these parameters.

Specificity of REM-sleep delta waves with respect to wakefulness. In order to verify whether delta waves of REM sleep are specific of this stage or may also be observed in wakefulness, additional analyses were performed using REM and waking (rest with eyes closed) data collected in 12 healthy adults (6 females, age 25.5 3.7; Bernardi et al., submitted). These recordings were preprocessed as previously described, but a 0.5-45 Hz bandpass filter was used in this case. Moreover, resting state recordings in wakefulness were initially divided into non-overlapping 5 s epochs and visually inspected to identify and reject epochs containing clear artifacts, before application of the ICA procedure. A non-parametric Wilcoxon signed rank test was used to compare amplitude and density of delta waves across REM-sleep and wakefulness.

Source modeling analysis. A source modeling analysis was performed to determine the cortical involvement of delta waves in REM-sleep. First, the negative-going envelope of the EEG signal was obtained by selecting the second most negative sample across 65 channels included in a medial fronto-central or in a temporo-occipital region of interest (ROI) (Siclari et al., 2014; Mensen et al., 2016). The resulting signal was broadband filtered (0.5-40 Hz, stop-band at 0.1 and 60 Hz) and the same negative half-wave detection algorithm described above was applied. Specific criteria were applied to further select waves with typical properties of fronto-central and medial-occipital waves, respectively, and to optimize source estimation while minimizing the potential impact of residual noise. In particular, anterior waves with a negative amplitude greater than 20 μV and a duration of 125-375 ms, and posterior waves with a negative amplitude of 5-50 μV and a duration >300 ms were

analyzed. The duration ranges applied here were broader than those reported for the other analyses at the single-channel level in order to take into account potential wave propagation (Massimini et al., 2004; Mensen et al., 2016). For the analysis of fronto-central waves, the EEG signal was filtered between 2 and 5 Hz (stop-band at 1.5 and 6 Hz), while it was filtered between 0.5 and 2.5 Hz (stop-band at 0.1 and 4 Hz) for medial-occipital waves. Then, source localization was performed on 1s data segments centered on the negative peak of each delta wave using GeoSource (NetStation, Electrical Geodesics, Inc). A four-shell head model based on the Montreal Neurological Institute (MNI) atlas and a standard coregistered set of electrode positions were used to construct the forward model. The inverse matrix was computed using the standardized low-resolution brain electromagnetic tomography (sLORETA) constraint. A Tikhonov regularization procedure (10^{-2}) was applied to account for the variability in the signal-to-noise ratio. The source space was restricted to 2,447 dipoles distributed over 7 mm^3 cortical voxels. For each delta wave, the cortical involvement was computed as the average of the relative current density achieved within a time-window of 20 ms around the wave negative peak. Finally, for each subject, the probabilistic involvement was defined as the probability for each voxel to be among the 25% of voxels showing the maximal cortical involvement.

Experimental Design and Statistical Analysis. All statistical analyses were performed using MATLAB (TheMathWorks, Inc.) or SPSS Statistics (IBM Corp., Armonk, N.Y., USA).

Statistical comparisons between phasic and tonic REM periods or between pre- and post-EM periods were performed using parametric paired t-tests including all study participants (N=16; Madison Dataset). The relationship between the number of delta waves and the number of rapid EMs was investigated using the Spearman's correlation coefficient. A non-parametric, permutation-based test was used to evaluate significance of overnight amplitude and density changes in delta waves. Non-parametric Friedman's tests were applied to identify potential differences across sleep stages (N2, N3, REM), while Wilcoxon signed rank tests were used for paired comparisons with relatively small sample sizes (N=10, or N=12).

When hypotheses were tested across multiple voxels/electrodes, a non-parametric approach based on the definition of a cluster-size-threshold was used to control for multiple comparisons (Nichols and Holmes, 2002; Fattinger et al., 2017). Specifically, a null distribution was generated by randomly relabeling the condition-label from the original data for group-level comparisons and by randomly reordering observations for correlation analyses (N permutations = 1,000). For each permutation, the maximal size of the resulting clusters reaching an (uncorrected) significance threshold of $p < 0.05$ were included in the cluster-size distribution. Then, the 95th percentile (5% significance level) was determined as the critical cluster-size threshold.

Results

Topographic analysis of delta waves in REM-sleep. First, we evaluated the topographic distribution of the density, amplitude, duration and negative peaks of all negative waves detected in the 1-4 Hz range (Figure 1A). We identified two spatially distinct clusters with different properties: i) a fronto-central cluster, in which waves had a relatively high density, a high amplitude, a low duration and a low number of negative peaks, and ii) a medial-occipital cluster characterized by fewer waves, with a lower amplitude, a longer duration and a higher number of negative peaks. Next, we

selected a representative electrode for each of the two clusters (channel 8, corresponding to the channel between Fz and Cz, and channel 137, corresponding to Oz), and compared the distribution of wave density as a function of their duration between the two channels (Figure 1B, left part). This analysis confirmed that the frontal cluster contained more faster waves (125 to 250 ms, >2 Hz), while the medial-occipital cluster contained more slower waves (300 to 500 ms, <2 Hz). Mean values for density, amplitude and negative peaks for characteristic faster fronto-central waves (125-250 ms) and slower medial-occipital waves (300 to 500 ms) are shown in Figure 1B (right part). Next, to better characterize the temporal dynamics of the occurrence of delta waves, we evaluated the topographic distribution of wave parameters only for delta waves occurring in bursts (see Methods for details). This analysis revealed that waves occurring in bursts were mainly found in the fronto-central cluster and had similar characteristics to the fronto-central waves described above (Figure 2). For subsequent analyses, we distinguished between fronto-central faster waves lasting 125-250 ms, and medial-occipital slower waves lasting 300-500 ms. We found that both types of waves were essentially local, as indicated by the mean proportion of recruited channels (32.0 ± 4.0% for fronto-central waves and 9.5 ± 3.5% for medial-occipital waves; Figure 3) and by the low probability of simultaneous detections in the fronto-central and in the medial-occipital electrode (15.2 ± 5.0% and 4.6 ± 3.5%, respectively). Importantly, faster fronto-central and slower medial-occipital waves tended to occur independently from each other: for each wave type, co-occurrence with the other wave type across the fronto-central and the medial-occipital electrode was observed for only 4.9 ± 1.3% and 16.4 ± 4.3% of all delta waves, respectively. Given that the observed values are closer to 0% than to 100%, our results suggest the existence of distinct generators for the two wave types.

[Figure 1]

[Figure 2]

[Figure 3]

Faster fronto-central waves ('sawtooth waves'). Visual inspection of these waves revealed that many of them looked like typical '*sawtooth waves*' of REM-sleep (Figure 4A), displaying a notch either before or after the maximum negative peak. These waves showed a frequency peak between 2.5 and 3 Hz and a maximum power between the vertex (Cz) and frontal (Fz) electrodes (Figure 4A-B). It should be noted that in some studies, sawtooth waves are described as having a positive polarity (i.e., recognizing the positive component as prominent; (Yasoshima et al., 1984; Sato et al., 1997)) while others have regarded sawtooth waves as negative waves (Terzano et al., 1997; Rodenbeck et al., 2006). In fact, sawtooth waves often present a relatively symmetrical distribution around the zero voltage baseline. In the present work, only negative half-waves were specifically included (Terzano et al., 1997; Rodenbeck et al., 2006). Source modeling of the signal corresponding to the maximum negative peak revealed the greatest overlap between subjects (>10) in a medial frontal area comprising the mid-cingulate gyrus, the supplementary motor area (SMA) and the medial part of the primary motor (M1) cortex (Figure 4C). Sawtooth waves displayed a clear density increase before rapid EM and during phasic REM periods (Figure 4D), in line with previous observations in both human subjects and primates (Berger et al.,

1962; Schwartz, 1962; Snyder et al., 1978; Sato et al., 1997; Pearl et al., 2002; Takaharaa et al., 2009). A direct positive correlation between the number of sawtooth waves preceding the EMs and the number of associated EMs was also observed (Figure 5). Finally, the analysis of *gamma* activity during sawtooth waves revealed a positive, in-phase, association between low- and high-frequency EEG activity (Figure 4E).

[Figure 4]

[Figure 5]

Next, given the notched appearance of typical sawtooth waves (Rodenbeck et al., 2006), we evaluated the topographic and cortical distribution of the signal during the notch and maximum negative peak of the wave separately. Specifically, for each detected wave presenting characteristics of sawtooth waves, we visually identified the timing of the most prominent secondary peak occurring on the negative slope (from positive to negative) of the wave. This analysis, applied at the scalp and source level revealed that the notched appearance results from the superimposition of two cortical sources: a fronto-central source corresponding to the maximal negative peak of the sawtooth wave, involving the mid-cingulate, medial and superior frontal areas (including motor and premotor regions), and a posterior source, corresponding to the notch of the wave, involving occipital and inferior temporo-occipital areas. Results of one representative subject are shown in Figure 6. For consistency, only sawtooth waves with a notch preceding the maximum negative peak were visually identified for this analysis although sometimes, a notch could also be observed following the maximum negative peak.

[Figure 6]

Slow medial-occipital waves. Visual inspection of EEG traces revealed that the great majority of slow (300-500 ms) medial-occipital waves corresponded to shallow negative deflections, frequently accompanied by faster, superimposed theta-alpha activity (Figure 7A). These waves showed their maximum power in the occipital cortex (Figure 7A-C) and did not display clear changes in relation to rapid EM. However, they showed a relative decrease in fronto-central, but not in occipital areas during phasic vs. tonic REM-sleep periods (Figure 7D). Similar to slow waves in NREM-sleep (e.g., (Siclari et al., 2014)), REM slow waves were associated with a decrease in gamma activity (Figure 7E).

[Figure 7]

Overnight changes in delta waves. An analysis of overnight changes in wave amplitude revealed a significant, non-region-specific (i.e., both frontal and occipital) and non-frequency-specific (i.e., for both faster and slower waves) decrease across the night (Figure 8). No overnight changes in wave density were observed.

[Figure 8]

Relationship with delta waves of NREM sleep. We then asked whether waves with 'sawtooth' and 'medial-occipital' characteristics were specific to REM-sleep or whether they could also occur in NREM-sleep. We found that the density of delta waves in the sawtooth frequency range differed significantly between stages (Friedman test $p < 0.0001$, $X^2 = 20.0$) in the fronto-central region, being maximal in REM-sleep, and lowest in N3-sleep ($p < 0.005$, $|z| = 2.803$; Wilcoxon signed-rank test). Instead, the density of slower waves in the medial-occipital cluster did not change significantly across sleep stages (Friedman test $p > 0.05$, $X^2 = 5.4$; Figure 9). Amplitude was significantly higher in N2 and N3 sleep than in REM-sleep for both faster fronto-central waves (Friedman test $p < 0.0001$, $X^2 = 16.8.0$) and slower medial-occipital waves (Friedman test $p < 0.0001$, $X^2 = 20.0$). For a topographic display of waves across stages, see Figure 10.

[Figure 9]

[Figure 10]

Relationship with delta waves of wakefulness. Because we found that the slower medial occipital waves were not specific to REM-sleep, but also occurred with a similar incidence in NREM-sleep, we asked whether they were also present in wakefulness. To this aim we performed an additional analysis in a different dataset, containing both REM-sleep and wake data (2 min of relaxed wakefulness obtained with eyes closed in the morning). This analysis showed that medial-occipital slow waves had a significantly lower density ($p < 0.005$, $|z| = 3.059$) in wakefulness relative to REM-sleep. Specifically, the average density was 5.5 ± 2.8 w/min in awake subjects, and 14.1 ± 1.6 w/min during REM-sleep (across the whole night), suggesting that they are clearly modulated by the change in behavioral state (sleep vs. wakefulness). Wave amplitude was similar across conditions ($p = 0.272$, $|z| = 1.098$). The same analysis performed for faster, fronto-central waves showed that these waves had a higher density ($p < 0.005$, $|z| = 3.059$) and amplitude ($p < 0.005$, $|z| = 2.903$) in REM-sleep relative to wakefulness. The average density of fronto-central waves was 34.0 ± 4.7 w/min in awake subjects, and 54.1 ± 7.1 w/min during REM-sleep.

Discussion

Here we show that delta waves (≤4 Hz) are an integral part of human REM-sleep. By analyzing delta wave properties separately, two distinct spatial clusters emerged spontaneously: a frontal-central cluster with frequent, faster (2-4 Hz) high-amplitude waves and a medial-occipital cluster with isolated, slower (<2 Hz), low-amplitude waves. Both waves were essentially local, involving only a minority of channels, and occurred independently from one another.

Fronto-central sawtooth waves. These waves resembled typical sawtooth waves of REM sleep, originally described in the 1960s (Jouvet et al., 1960; Schwartz and Fischgold, 1960; Berger et al., 1962). There is no universal agreement on defining criteria for sawtooth waves, but they are often described as medium amplitude waves (≥ 20 μV) between 2 and 5 Hz (Jouvet et al., 1960; Berger et al., 1962; Yasoshima et al., 1984; Pinto Jr et al., 2002; Vega-Bermudez et al., 2005), with a triangular shape (initial slow increase followed by a steep decrease (Rechtschaffen and Kales, 1968; Tafti et al., 1991; Rodenbeck et al., 2006)), and a maximal fronto-central amplitude (Yasoshima et al., 1984; Broughton and Hasan, 1995). The presence of a notch, usually on the positive-to-negative slope, is occasionally mentioned (Foulkes and Pope, 1973; Rodenbeck et al., 2006). Sawtooth waves tend to occur in bursts (Geisler et al., 1987; Sato et al., 1997), herald the beginning of REM-sleep (Sato et al., 1997) and often, but not necessarily accompany bursts of rapid EMs (Berger et al., 1962; Schwartz, 1962; Sato et al., 1997; Takaharaa et al., 2009). The characteristics of fronto-central waves described herein are consistent with these observations. In addition, we provide several novel findings. First, using source modeling, we demonstrate a maximal involvement in medial prefrontal areas (mid-cingulate cortex, SMA and the medial M1). We also identified a secondary temporo-occipital source, associated with the sawtooth wave 'notch'. Second, we showed that sawtooth waves are accompanied by an (in-phase) increase in high-frequency activity, suggesting an 'activating' effect (i.e., increased neuronal firing (Steriade et al., 1996)). The mechanism underlying these waves is thus likely different from NREM slow waves, which are associated with neuronal silence (*OFF-periods*). Finally, we were able to document a direct correlation between sawtooth waves and rapid EMs (the more sawtooth waves, the more subsequent EMs).

The characteristics of sawtooth waves raise the possibility that they are related to ponto-geniculo-occipital (PGO) waves, which were originally described in cats and consist of phasic electric potentials recorded from the pons, the lateral geniculate body (LGB), and the occipital cortex (Jouvet and Michel, 1959; Mikiten, 1961; Brooks and Bizzi, 1963; Mouret et al., 1963). They have also been mapped in limbic areas (amygdala, cingulate cortex and hippocampus). Similar to sawtooth waves, PGO waves last between 60 and 360 ms (Callaway et al., 1987), appear at the NREM-REM sleep transition, several seconds before the first rapid EM (Sato et al., 1997), occur in bursts (but isolated spikes are also observed (Jeannerod and Kiyono, 1969)), and are typically, but not always associated with trains of EMs (Morrison and Pompeiano, 1966). Although PGO waves have been recorded in many species, including nonhuman primates, their existence in humans remains controversial. A relation between sawtooth and PGO waves has been suggested based on the similar temporal characteristics, including their association with rapid EMs (Ishiguro et al., 1979; Takaharaa et al., 2009), but the different cortical distributions (fronto-central vs occipital) have hampered further analogies. The temporo-occipital component that we identified here may actually represent the cortical manifestation of human PGO waves. The increases in gamma power associated with sawtooth waves fit well with this hypothesis. Indeed, PGO waves have been referred to as 'cortical activation waves' (Calvet and Calvet, 1968) because they are associated with increased neuronal firing in several cortical regions. Consistent with our findings, gamma power increases have been reported during rapid EM in frontal and central regions in REM sleep (Abe et al., 2008; Vijayan et al., 2017) and during phasic compared to tonic REM sleep (Corsi-Cabrera et al., 2008). Among the few case studies documenting

potential human PGO-wave equivalents using intracranial recordings (Salzarulo et al., 1975; Lim et al., 2007; Fernández-Mendoza et al., 2009), one described the presence of simultaneous sawtooth waves in the scalp EEG, in addition to increases in gamma activity (15-35 Hz), supporting the analogy between sawtooth and PGO waves (Fernández-Mendoza et al., 2009).

The correlation between sawtooth waves and rapid EM raises the question of whether sawtooth waves are directly involved in rapid EM generation. However, several points argue against this possibility. First, although saccades during wakefulness and REM sleep share many common features, including analogous ERP waveforms, the same phase reset of theta activity in medial temporal regions, a comparable modulation of neuronal firing rates (Andrillon et al., 2015) and the activation of similar brain regions (Hong et al., 1995; Ioannides et al., 2004), sawtooth waves do not accompany rapid EM during wakefulness. Second, while sawtooth waves clearly encompass the frontal and supplementary eye field, they also extend beyond these regions, to V1, the SMA and limbic regions (midcingulate, inferior/middle temporal cortex). Activations of these areas (Maquet et al., 1996; Nofzinger et al., 1997; Braun et al., 1998; Ioannides et al., 2004; Abe et al., 2008) and the LGB (Peigneux et al., 2001; Wehrle et al., 2005; Miyauchi et al., 2009) have been shown to differentiate brain activity during REM sleep from EM during wakefulness (Peigneux et al., 2001; Miyauchi et al., 2009). Our results suggest that these differences may be mediated by sawtooth waves, which are concomitant to EMs. Finally, the fronto-central topography is almost identical to some NREM potentials that are not associated with EMs, including vertex waves (Yasoshima et al., 1984; Siclari et al., 2014) and high-frequency activity increases following type I slow waves (Siclari et al., 2014, 2018; Bernardi et al., 2018). During wakefulness, vertex potentials can be induced by sudden and intense stimuli of various sensory modalities, including pain. These potentials have been suggested to be related to stimulus saliency, that is, the ability of a stimulus to stand out from its surroundings (Legrain et al., 2011). Rapid EMs following sawtooth waves may thus constitute a reaction to a salient, possibly dreamt event. Consistent with this, PGO spikes can be induced in cats using sounds, during both quiet wakefulness, REM and NREM sleep, and may accompany a 'startle-like' reaction (Bowker and Morrison, 1976), suggesting common behavioral significance of these potentials across states.

Future studies should explore the relationship between sawtooth waves and midline frontal rhythms in the delta and theta frequency range that have been linked to cognitive processes during wakefulness and are phase coupled to gamma oscillations (Gevins et al., 1997; Sauseng et al., 2010; Fujisawa and Buzsáki, 2011). Also, given the prominent inferior temporal component of sawtooth waves, it would be of interest to evaluate how sawtooth waves relate to hippocampal delta rhythms of REM-sleep that have been suggested to represent the human counterpart of hippocampal theta of mammalian REM sleep (Bódizs et al., 2001; Clemens et al., 2009; Moroni et al., 2012).

Medial-occipital slow waves. The second cluster of delta waves consisted of occipital slow waves (<2 Hz). This finding is consistent with previous work, describing the maximal peak of low-*delta* activity in occipital areas during REM-sleep (e.g., (Tinguely et al., 2006; Ferrara and De Gennaro, 2011)). Our results demonstrate that this source of *delta* activity is due to small, local slow waves that are

not modulated by phasic REM and are associated with a suppression of gamma activity, similar to NREM slow waves (e.g., (Siclari et al., 2014)). We also show, for the first time, that occipital slow waves occur with a similar density, but different amplitudes, across all sleep stages. The amplitude of delta waves was higher in N3 relative to N2 or REM sleep and decreased across subsequent REM-sleep periods. These variations may reflect neuromodulatory and sleep-dependent changes in synaptic density/strength which may affect the efficiency of neural synchronization during the generation and spreading of slow waves (Riedner et al., 2007; Tononi and Cirelli, 2014). On the other hand, occipital slow wave density remained similar in NREM and REM sleep, but was higher than in wakefulness. Consistent with this, the occipital cortex, relative to other cortical areas, shows the smallest changes in SWA at NREM-REM sleep transitions (De Gennaro et al., 2002; Ferrara and De Gennaro, 2011). The relatively low frequency of occipital REM slow waves (<2 Hz) is in line with the recent observation of a lower frequency of occipital NREM slow waves (~1 Hz) relative to anterior areas (Bersagliere et al., 2017).

Our observation of local occipital slow waves occurring at a similar rate across NREM and REM-sleep is consistent with the hypothesis that slow waves in primary cortices play a role in sensory disconnection during sleep (Funk et al., 2016). However, with respect to slow waves recently described in mice (Funk et al., 2016), several differences should be noted. First, we did not observe SWA peaks in primary cortices other than V1. It is possible that local slow waves in other primary cortices may have been masked by the preponderant sawtooth activity in these areas. Indeed, in a recent study comparing SWA between REM and wakefulness, SWA activity was found to be higher in primary sensory cortices in REM sleep after excluding sawtooth waves (Baird et al., 2018). This possibility is also in part supported by the observation of a relative decrease in the fronto-central wave density in the 1-2 Hz range during REM periods dominated by 'activating' sawtooth waves (i.e., phasic REM). Consistent with this view, recent work in animal models also described in REM-sleep a 4 Hz prefrontal oscillation that was modulated separately from a <2 HZ oscillation after chronic sleep restriction (Kim et al., 2017). Second, in our study we found that occipital slow waves, as opposed to sawtooth waves, were not modulated by phasic REM-periods like in the animal study. This may be due to the different definitions of phasic REM periods that were used, based on rapid EMs in humans and on whisking events (vibrissal EMG) in mice. However, we cannot exclude that slow waves observed in these two studies may represent distinct phenomena.

In several key aspects, these findings parallel the recent observation of two distinct slow wave populations of in NREM sleep: widespread fronto-central type I slow waves, temporally related to high-frequency increases (micro-arousals), and diffusely distributed, local type II slow waves that do not seem to be related to arousal systems (Siclari et al., 2014, 2018; Bernardi et al., 2018; Spiess et al., 2018). Thus both REM and NREM sleep appear to be characterized by fronto-central, potentially 'activating' delta waves that stand out from the background of remaining of slow waves.

Limitations. We focused on a minority of delta waves that were typical of clusters emerging from topographical analyses. Thus, there is a large 'unclassified' background of delta waves that remains unexplored in the present study. Due to volume conduction affecting scalp EEG recordings, masking effects of prominent sawtooth waves with respect to other slow waves could not be avoided. Future human

studies using intracranial recordings should explore the regional distribution of slow waves in REM sleep (primary vs. secondary sensory cortices) and their association with *off-periods*.

Conclusions. Delta waves (≤4 Hz) are an integral feature of REM-sleep. There appear to be at least two distinctive clusters of delta waves with different properties: a fronto-central cluster characterized by faster, activating 'sawtooth waves' that share many characteristics with PGO waves described in animals, and a medial-occipital cluster containing slow waves which are more similar to NREM sleep slow waves.

References

Abe T, Ogawa K, Nittono H, Hori T (2008) Neural generators of brain potentials before rapid eye movements during human REM sleep: a study using sLORETA. Clin Neurophysiol 119:2044–2053.

Andrillon T, Nir Y, Cirelli C, Tononi G, Fried I (2015) Single-neuron activity and eye movements during human REM sleep and awake vision. Nat Commun 6.

Aserinsky E, Kleitman N (1953) Regularly occurring periods of eye motility, and concomitant phenomena, during sleep. Science (80-) 118:273–274.

Baird B, Castelnovo A, Riedner BA, Lutz A, Ferrarelli F, Boly M, Davidson RJ, Tononi G (2018) Human Rapid Eye Movement Sleep Shows Local Increases in Low-Frequency Oscillations and Global Decreases in High-Frequency Oscillations Compared to Resting Wakefulness. Eneuro:ENEURO.0293-18.2018.

Berger RJ, Olley P, Oswald I (1962) The EEG, eye-movements and dreams of the blind. Q J Exp Psychol 14:183–186.

Bernardi G, Betta M, Cataldi J, Leo A, Haba-Rubio J, Heinzer R, Cirelli C, Tononi G, Pietrini P, Ricciardi E, Siclari F (submitted) Visual imagery and visual perception induce similar changes in occipital slow waves of sleep.

Bernardi G, Siclari F, Handjaras G, Riedner BA, Tononi G (2018) Local and Widespread Slow Waves in Stable NREM Sleep : Evidence for Distinct Regulation Mechanisms. Front Hum Neurosci 12:1–13.

Bernardi G, Siclari F, Yu X, Zennig C, Bellesi M, Ricciardi E, Cirelli C, Ghilardi MF, Pietrini P, Tononi G (2015) Neural and behavioral correlates of extended training during sleep deprivation in humans: evidence for local, task-specific effects. J Neurosci 35:4487–4500.

Bersagliere A, Pascual-Marqui RD, Tarokh L, Achermann P (2017) Mapping Slow Waves by EEG Topography and Source Localization: Effects of Sleep Deprivation. Brain Topogr:1–13.

Betta M, Gemignani A, Landi A, Laurino M, Piaggi P, Menicucci D (2013) Detection and removal of ocular artifacts from EEG signals for an automated REM sleep analysis. In: 2013 35th Annual International Conference of the IEEE Engineering in Medicine and Biology Society (EMBC), pp 5079–5082. IEEE.

Betta M, Laurino M, Gemignani A, Landi A, Menicucci D (2015) A Classification method for eye movements direction during REM sleep trained on wake electro-oculographic recordings. In: 2015 37th Annual International Conference of the IEEE Engineering in Medicine and Biology Society (EMBC), pp 370–373. IEEE.

Bódizs R, Kántor S, Szabó G, Szûcs A, Erõss L, Halász P (2001) Rhythmic hippocampal slow oscillation characterizes REM sleep in humans. Hippocampus 11:747–753.

Bowker RM, Morrison AR (1976) The startle reflex and PGO spikes. Brain Res 102:185–190.

Braun AR, Balkin TJ, Wesensten NJ, Gwadry F, Carson RE, Varga M, Baldwin P, Belenky G, Herscovitch P (1998) Dissociated pattern of activity in visual cortices and their projections during human rapid eye movement sleep. Science 279:91–95.

Brooks DC, Bizzi E (1963) Brain stem electrical activity during sleep. Arch Ital Biol 101:648–665.

Broughton R, Hasan J (1995) Quantitative Topographic Electroencephalographic Mapping During Drowsiness and Sleep Onset. J Clin Neurophysiol 12:372–386.

Callaway CW, Lydic R, Baghdoyan HA, Hobson JA (1987) Pontogeniculooccipital waves: Spontaneous visual system activity during rapid eye movement sleep. Cell Mol Neurobiol 7:105–149.

Calvet J, Calvet M-C (1968) Étude quantitative et organisation en fonction de la vigilance de l'activitéunitaire des diverses régions du cortex cérébral. Brain Res 10:183–199.

Clemens Z, Weiss B, Szűcs A, Erőss L, Rásonyi G, Halász P (2009) Phase coupling between rhythmic slow activity and gamma characterizes mesiotemporal rapid-eye-movement sleep in humans. Neuroscience 163:388–396.

Corsi-Cabrera M, Guevara MA, del Río-Portilla Y (2008) Brain activity and temporal coupling related to eye movements during REM sleep: EEG and MEG results. Brain Res 1235:82–91.

De Gennaro L, Ferrara M, Curcio G, Cristiani R, Bertini M (2002) Cortical EEG topography of REM onset: the posterior dominance of middle and high frequencies. Clin Neurophysiol 113:561–570.

Delorme A, Makeig S (2004) EEGLAB: an open source toolbox for analysis of single-trial EEG dynamics including independent component analysis. J Neurosci Methods 134:9–21.

Dement W, Kleitman N (1957) Cyclic variations in EEG during sleep and their relation to eye movements, body motility, and dreaming. Electroencephalogr Clin Neurophysiol 9:673–690.

Fattinger S, Kurth S, Ringli M, Jenni OG, Huber R (2017) Theta waves in children's waking electroencephalogram resemble local aspects of sleep during wakefulness. Sci Rep 7:11187.

Fernández-Mendoza J, Lozano B, Seijo F, Santamarta-Liébana E, José Ramos-Platón M, Vela-Bueno A, Fernández-González F (2009) Evidence of Subthalamic PGO-like Waves During REM Sleep in Humans: a Deep Brain Polysomnographic Study. Sleep 32:1117–1126.

Ferrara M, De Gennaro L (2011) Going local: insights from EEG and stereo-EEG studies of the human sleep-wake cycle. Curr Top Med Chem 11:2423–2437.

Foulkes D, Pope R (1973) Primary visual experience and secondary cognitive elaboration in stage REM: a modest confirmation and an extension. Percept Mot Ski 37:107–118.

Fujisawa S, Buzsáki G (2011) A 4 Hz Oscillation Adaptively Synchronizes Prefrontal, VTA, and Hippocampal Activities. Neuron 72(1), 153-165.

Funk CM, Honjoh S, Rodriguez A V, Cirelli C, Tononi G (2016) Local Slow Waves in Superficial Layers of Primary Cortical Areas during REM Sleep. Curr Biol 26:396–403.

Geisler P, Meier-Ewert K, Matsubayshi K (1987) Rapid eye movements, muscle twitches and sawtooth waves in the sleep of narcoleptic patients and controls. Electroencephalogr Clin Neurophysiol 67:499–507.

Gevins A, Smith ME, McEvoy L, Yu D (1997) High-resolution EEG mapping of cortical activation related to working memory: Effects of task difficulty, type of processing, and practice. Cereb Cortex 7(4), 374-385.

Hong CC, Gillin JC, Dow BM, Wu J, Buchsbaum MS (1995) Localized and lateralized cerebral glucose metabolism associated with eye movements during REM sleep and wakefulness: a positron emission tomography (PET) study. Sleep 18:570–580.

Huber R, Ghilardi MF, Massimini M, Ferrarelli F, Riedner BA, Peterson MJ, Tononi G (2006) Arm immobilization causes cortical plastic changes and locally decreases sleep slow wave activity. Nat Neurosci 9:1169.

Huber R, Ghilardi MFFFF, Massimini M, Tononi G (2004) Local sleep and learning. Nature 430:78–81.

Hung C-S, Sarasso S, Ferrarelli F, Riedner B, Ghilardi MF, Cirelli C, Tononi G (2013) Local experience-dependent changes in the wake EEG after prolonged wakefulness. Sleep 36:59–72.

Iber C, Ancoli-Israel S, A C (2007) The AASM manural for the scoring of sleep and associated events: Rules, terminology and technical specifications. Rules, Terminology and Technical Specifications, Darien, Illinois, American Academy of Sleep Medicine.

Ioannides AA, Corsi-Cabrera M, Fenwick PBC, del Rio Portilla Y, Laskaris NA, Khurshudyan A, Theofilou D, Shibata T, Uchida S, Nakabayashi T (2004) MEG tomography of human cortex and brainstem activity in waking and REM sleep saccades. Cereb Cortex 14:56–72.

Ishiguro T, Hanamura S, Otaka T (1979) The saw-tooth wave associated with small nystagmus: a study on a narcoleptic patient and her family. Sleep Res 8:195.

Jeannerod M, Kiyono S (1969) Unitary discharge of pontine reticular formation and phasic ponto-geniculo-occipital activity in the cat under reserpine. Brain Res 12:112–128.

757 Johns MW (1991) A new method for measuring daytime sleepiness: the Epworth sleepiness
758 scale. Sleep 14:540–545.
759 Jouvet M, Michel F (1959) Corrélations électromyographiques du sommeil chez le chat
760 décortiqué et mésencéphalique chronique. Comptes Rendus la Socie´te´ Biol 153:422–
761 425.
762 Jouvet M, Michel F, Mounier D (1960) Analyse électroencéphlographique comparée du
763 sommeil physiologique chez le chat et chez l'homme. Rev Neurol (Paris) 103:189–204.
764 Kim B, Kocsis B, Hwang E, Kim Y, Strecker RE, McCarley RW, Choi JH (2017) Differential
765 modulation of global and local neural oscillations in REM sleep by homeostatic sleep
766 regulation. Proc Natl Acad Sci 114(9), E1727-E1736.
767 Legrain V, Iannetti GD, Plaghki L, Mouraux A (2011) The pain matrix reloaded: a salience
768 detection system for the body. Prog Neurobiol 93:111–124.
769 Lim AS, Lozano AM, Moro E, Hamani C, Hutchison WD, Dostrovsky JO, Lang AE,
770 Wennberg RA, Murray BJ (2007) Characterization of REM-sleep associated ponto-
771 geniculo-occipital waves in the human pons. Sleep 30:823–827.
772 Maquet P, Péters J-M, Aerts J, Delfiore G, Degueldre C, Luxen A, Franck G (1996)
773 Functional neuroanatomy of human rapid-eye-movement sleep and dreaming. Nature
774 383:163–166.
775 Massimini M, Huber R, Ferrarelli F, Hill S, Tononi G (2004) The Sleep Slow Oscillation as a
776 Traveling Wave. J Neurosci 24:6862–6870.
777 Mensen A, Riedner B, Tononi G (2016) Optimizing detection and analysis of slow waves in
778 sleep EEG. J Neurosci Methods 274:1–12.
779 Mikiten T (1961) EEG desynchronization during behavioral sleep associated with spike
780 discharges from the thalamus of the cat. In: Fed. Proc., pp 327.
781 Miyauchi S, Misaki M, Kan S, Fukunaga T, Koike T (2009) Human brain activity time-
782 locked to rapid eye movements during REM sleep. Exp Brain Res 192:657–667.
783 Moroni F, Nobili L, De Carli F, Massimini M, Francione S, Marzano C, Proserpio P, Cipolli
784 C, De Gennaro L, Ferrara M (2012) Slow EEG rhythms and inter-hemispheric
785 synchronization across sleep and wakefulness in the human hippocampus. Neuroimage
786 60:497–504.
787 Morrison AR, Pompeiano O (1966) Vestibular influences during sleep. IV. Functional
788 relations between vestibular nuclei and lateral geniculate nucleus during desynchronized
789 sleep. Arch Ital Biol 104:425.
790 Mouret J, Jeannerod M, Jouvet M (1963) L'activite electrique du systeme visuel au cours de
791 la phase paradoxale du sommeil chez le chat. J Physiol 55:305–306.
792 Nichols TE, Holmes AP (2002) Nonparametric permutation tests for functional
793 neuroimaging: A primer with examples. Hum Brain Mapp 15:1–25.
794 Nir Y, Staba RJ, Andrillon T, Vyazovskiy V V., Cirelli C, Fried I, Tononi G (2011) Regional
795 Slow Waves and Spindles in Human Sleep. Neuron 70:153–169.
796 Nofzinger EA, Mintun MA, Wiseman M, Kupfer DJ, Moore RY (1997) Forebrain activation
797 in REM sleep: an FDG PET study. Brain Res 770:192–201.
798 Pearl PL, LaFleur BJ, Reigle SC, Rich A-S, Freeman AAH, McCutchen C, Sato S (2002)
799 Sawtooth wave density analysis during REM sleep in normal volunteers. Sleep Med
800 3:255–258.
801 Peigneux P, Laureys S, Fuchs S, Delbeuck X, Degueldre C, Aerts J, Delfiore G, Luxen A,
802 Maquet P (2001) Generation of rapid eye movements during paradoxical sleep in
803 humans. Neuroimage 14:701–708.
804 Pinto Jr LR, Peres C de A, Russo RH, Remesar-Lopez AJ, Tufik S (2002) Sawtooth waves
805 during REM sleep after administration of haloperidol combined with total sleep
806 deprivation in healthy young subjects. Brazilian J Med Biol Res 35:599–604.
807 Rechtschaffen A, Kales A (1968) A manual of standardized terminology, techniques and
808 scoring system for sleep stages of human subjects. Allan Rechtschaffen and Anthony
809 Kales, editors (Rechtschaffen A, Kales A, University of California LABIS, Network
810 NNI, eds). Bethesda, Md: U. S. National Institute of Neurological Diseases and
811 Blindness, Neurological Information Network.

812 Riedner BA, Vyazovskiy V V, Huber R, Massimini M, Esser S, Murphy M, Tononi G (2007)
813 Sleep homeostasis and cortical synchronization: III. A high-density EEG study of sleep
814 slow waves in humans. Sleep 30:1643.
815 Rodenbeck A, Binder R, Geisler P, Danker-Hopfe H, Lund R, Raschke F, Weeß H, Schulz H
816 (2006) A review of sleep EEG patterns. Part I: a compilation of amended rules for their
817 visual recognition according to Rechtschaffen and Kales. Somnologie 10:159–175.
818 Salzarulo P, Pelloni G, Lairy G. (1975) Semeiologie electrophysiologique du sommeil de jour
819 chez l'enfant de 7 a 9 ans. Electroencephalogr Clin Neurophysiol 38:473–494.
820 Sato S, McCutchen C, Graham B, Freeman A, von Albertini-Carletti I, Alling DW (1997)
821 Relationship between muscle tone changes, sawtooth waves and rapid eye movements
822 during sleep. Electroencephalogr Clin Neurophysiol 103:627–632.
823 Sauseng P, Griesmayr B, Freunberger R, Klimesch W (2010) Control mechanisms in working
824 memory: A possible function of EEG theta oscillations. Neurosci Biobehav Rev 34(7),
825 1015-1022.
826 Schwartz BA (1962) EEG et mouvements oculaires dans le sommeil de nuit.
827 Electroencephalogr Clin Neurophysiol 14:126–128.
828 Schwartz BA, Fischgold H (1960) Introduction à l'étude polygraphique du sommeil de nuit
829 (mouvements oculaires et cycles de sommeil). Vie Medicale au Canada Français 41:39–
830 46.
831 Siclari F, Baird B, Perogamvros L, Bernardi G, LaRocque JJJJJ, Riedner B, Boly M, Postle
832 BRRRR, Tononi G (2017) The neural correlates of dreaming. Nat Neurosci 20:872–878.
833 Siclari F, Bernardi G, Cataldi J, Tononi G (2018) Dreaming in NREM sleep: a high-density
834 EEG study of slow waves and spindles. J Neurosci 38:0855-18.
835 Siclari F, Bernardi G, Riedner BA, LaRocque JJ, Benca RM, Tononi G (2014) Two Distinct
836 Synchronization Processes in the Transition to Sleep: A High-Density
837 Electroencephalographic Study. Sleep 37:1621–1637.
838 Siclari F, Tononi G (2017) Local aspects of sleep and wakefulness. Curr Opin Neurobiol
839 44:222–227.
840 Snyder EW, Dustman RE, Johnson RL (1978) Sawtooth waves: concomitants of rapid eye
841 movement sleep in monkeys. Electroencephalogr Clin Neurophysiol 45:111–113.
842 Spiess M, Bernardi G, Kurth SS, Ringli M, Wehrle FM, Jenni OG, Huber R, Siclari F, Wehrle
843 FM, Jenni OG, Huber R, Siclari F (2018) How do children fall asleep? A high-density
844 EEG study of slow waves in the transition from wake to sleep. Neuroimage 178:23–35.
845 Steriade M, Amzica F, Contreras D (1996) Synchronization of fast (30-40 Hz) spontaneous
846 cortical rhythms during brain activation. J Neurosci 16:392–417.
847 Steriade M, Nuñez A, Amzica F (1993) A novel slow (< 1 Hz) oscillation of neocortical
848 neurons in vivo: depolarizing and hyperpolarizing components. J Neurosci 13:3252–
849 3265.
850 Steriade M, Timofeev I, Grenier F (2001) Natural Waking and Sleep States: A View From
851 Inside Neocortical Neurons. J Neurophysiol 85:1969–1985.
852 Tafti M, Olivet H, Billiard M (1991) Phasic events in narcolepsy and sleep apnea syndrome.
853 Terzano, M G , P Hal A C Declerck (Ed) L E R S (Laboratoires D'etudes Rech
854 Synthelabo) Monogr Ser Vol 7 Phasic Events Dyn Organ Sleep; Second Int Work
855 Parma, Italy, May 1989 Xiii+210p Raven Press:151–166 Available at:
856 https://m.eurekamag.com/research/032/788/032788677.php [Accessed July 30, 2018].
857 Takaharaa M, Kanayamab S, Horib T (2009) Co-occurrence of Sawtooth Waves and Rapid
858 Eye Movements during REM Sleep. Int J Bioelectromagn 11:144–148.
859 Terzano M, Parrino L, Mennuni G (1997) Eventi Fasici e Microstruttura del Sonno/Phasic
860 events and microstructure of sleep (consensus conference) (Martano Editore, ed). Lecce,
861 Italy, Italy.
862 Tinguely G, Finelli LA, Landolt H-P, Borbély AA, Achermann P (2006) Functional EEG
863 topography in sleep and waking: state-dependent and state-independent features.
864 Neuroimage 32:283–292.
865 Tononi G, Cirelli C (2014) Sleep and the price of plasticity: from synaptic and cellular
866 homeostasis to memory consolidation and integration. Neuron 81:12–34.

867 Valderrama M, Crépon B, Botella-Soler V, Martinerie J, Hasboun D, Alvarado-Rojas C,
868 Baulac M, Adam C, Navarro V, Le Van Quyen M (2012) Human gamma oscillations
869 during slow wave sleep. PLoS One 7:e33477.
870 Vega-Bermudez F, Szczepanski S, Malow B, Sato S (2005) Sawtooth wave density analysis
871 during REM sleep in temporal lobe epilepsy patients. Sleep Med 6:367–370.
872 Vijayan S, Lepage KQ, Kopell NJ, Cash SS (2017) Frontal beta-theta network during REM
873 sleep. Elife 6.
874 Vyazovskiy V V, Cui N, Rodriguez A V, Funk C, Cirelli C, Tononi G (2014) The dynamics
875 of cortical neuronal activity in the first minutes after spontaneous awakening in rats and
876 mice. Sleep 37:1337–1347.
877 Vyazovskiy V V, Olcese U, Hanlon EC, Nir Y, Cirelli C, Tononi G (2011) Local sleep in
878 awake rats. Nature 472:443–447.
879 Wehrle R, Czisch M, Kaufmann C, Wetter TC, Holsboer F, Auer DP, Pollmächer T (2005)
880 Rapid eye movement-related brain activation in human sleep: a functional magnetic
881 resonance imaging study. Neuroreport 16:853–857.
882 Yasoshima A, Hayashi H, Iijima S, Sugita Y, Teshima Y, Shimizu T, Hishikawa Y (1984)
883 Potential distribution of vertex sharp wave and saw-toothed wave on the scalp.
884 Electroencephalogr Clin Neurophysiol 58:73–76.
885
886

887 **Figure/Table Legends**
888

889 *Table 1*. Sleep parameters (average and standard deviation) for the 16 subjects
890 included in the study.

891 *Figure 1*. Properties of delta waves in REM-sleep. An automatic detection algorithm
892 was applied to the EEG signal of each electrode to identify negative half-waves with a
893 duration of 125-500 ms (≤4 Hz). Different wave properties were extracted and
894 analyzed (panel A), including density (number of waves per minute; w/min), negative
895 amplitude (μV), duration (ms) and number of negative peaks (np/w). Of note, a
896 similar distribution was obtained for negative peaks when values were expressed 'per
897 second' instead of 'per wave', although highest values were found in more lateral
898 posterior, rather than medial posterior regions. Panel B (left) shows, for a fronto-
899 central and a medial-occipital electrode, the difference (%) in the relative proportion
900 of waves for durations between 125 and 500 ms (25 ms bins). The relative difference
901 between the two electrodes in % was calculated for each duration bin. Vertical bars
902 indicate one standard deviation from the group mean (SD). The table on the right side
903 displays mean values and SD for density, amplitude and negative peaks (neg. pks) for
904 the faster fronto-central and the slower medial-occipital delta waves.

905 *Figure 2*. Temporal distribution of delta waves (occurrence in bursts). Bursts were
906 defined as series of at least 3 consecutive waves (1-5 Hz) whose maximum negative
907 peaks were separated by less than 750 ms. From left to right, the plots display the
908 density of delta wave bursts (number of bursts per minute), the mean amplitude (μV)
909 and duration (ms) of waves included in a burst, and the number of waves included in
910 the burst (expressed as waves per burst).

911 *Figure 3*. Relationship between fronto-central and medial occipital delta waves. Panel
912 A shows the typical scalp involvement for the two types of delta waves. For each
913 delta wave detected in the two electrodes of interest (fronto-central and medial-
914 occipital), the number of concurrent detections (in a window of 200 ms, centered on
915 the wave negative peak) in other electrodes was computed. Thus, each map shows the
916 number of cases in which each electrode showed a co-occurring delta wave (the
917 electrode of interest has 100% value in each map). Panel B shows the relative
918 occurrence of simultaneous detections (of the same type/duration) across the two
919 electrodes of interest.

920 *Figure 4*. Panel A shows representative REM-sleep EEG traces (negative-up on the y-
921 scale) containing fronto-central delta waves with a duration of 125-250 ms (half-
922 wave). The orange dots indicate waves identified by the automatic detection
923 algorithm in the Cz electrode, while the red box marks the occurrence of eye
924 movements (EMs). Most waves corresponded to typical notched sawtooth waves of
925 REM-sleep. Panel B shows density- and power-based maps indicating their
926 topographic distribution. Power spectral density (PSD) was calculated in 6s epochs
927 and across all REM cycles using the Welch's method (8 sections, 50% overlap) and

integrated in the frequency-range of interest. Panel C shows the typical peak of activity of fronto-central waves in source space (overlap between subjects). Panel D shows a comparison between wave density before and after isolated eye movements and between phasic and tonic REM-periods. Panel E depicts the relationship between delta and gamma activity (RMS of band-limited signal). RMS traces were aligned using the maximum negative peak of each wave as a reference. * marks a significant increase of gamma activity at the wave peak with respect to baseline ($p < 0.05$).

Figure 5. Correlation between the number of sawtooth waves preceding rapid eye movements and the number of subsequent rapid eye movements. For each isolated group of eye movements, the burst of the 125-250 ms half-waves (amplitude > 10 μV, inter-wave distance < 1 s) closest to the beginning of the first eye movement (maximum distance < 600 ms) was identified. White dots mark significant effects at group level ($p < 0.05$, corrected).

Figure 6. Cortical sources of typical sawtooth waves. Panel A shows the EEG traces (three electrodes, corresponding to Fz, Cz, and Pz; negative-up on the y-scale) of two representative notched sawtooth waves (±250 ms around the negative peak of the algorithm detection). Panel B shows the scalp and cortical involvement corresponding to the notch and the maximal negative peak of a single sawtooth wave. Panel C shows the difference in average involvement between the notch and maximal negative peak (computed across 267 sawtooth waves in one representative subject, similar results were obtained in other participants). For this evaluation, all detections in one subject were visually inspected to identify typical sawtooth waves with a negative amplitude greater than 20 μV and a well-recognizable notched, triangular shape. The timing of the notch and the maximal negative peak were marked manually. Differences shown in Panel C are statistically significant over all voxels ($p<0.05$, corrected).

Figure 7. Panel A shows representative REM-sleep EEG traces (negative-up on the y-scale) containing medial-occipital delta waves with a duration of 300-500 ms (half-wave). The blue dot indicates a wave identified by the automatic detection algorithm in the Oz electrode. Panel B shows density- and power-based maps indicating their topographic distribution. Power spectral density (PSD) was calculated in 6 s epochs and across all REM cycles using the Welch's method (8 sections, 50% overlap) and integrated in the frequency-range of interest. Panel C shows the typical peak of activity of medial-occipital waves in source space (overlap between subjects). Panel D shows a comparison between medial-occipital wave density before and after isolated eye movements and between phasic and tonic REM-periods. Finally, panel E depicts the relationship between delta and gamma activity (RMS of band-limited signal). RMS traces were aligned using the maximum negative peak of each wave as a reference. * marks a significant decrease of gamma activity at the wave peak with respect to baseline ($p < 0.05$).

Figure 8. Overnight changes in the amplitude of delta waves in REM sleep for the 'sawtooth' frequency range (125-250 ms) and the medial-occipital wave range (300-

500 ms). A diffuse decrease in amplitude was observed for both frequency ranges. White dots mark significant effects at group level ($p < 0.05$, corrected).

Figure 9. Relative variations in the density and amplitude of fronto-central and medial-occipital delta waves in N2 and N3 with respect to REM sleep. The dashed red line corresponds to the level observed in REM sleep (100%). * denotes significant effects at $p < 0.05$ (red for Friedman test for stage-effect, black for post-hoc Wilcoxon signed rank tests).

Figure 10. Relative topographic distribution of EEG waves with durations of 125-250 ms (left) and 300-500 ms (right) in N2, N3 and REM sleep. Density values were z-scored to facilitate comparison across stages. The strong frontal slow wave activity in NREM sleep likely masks the smaller delta waves in posterior regions.

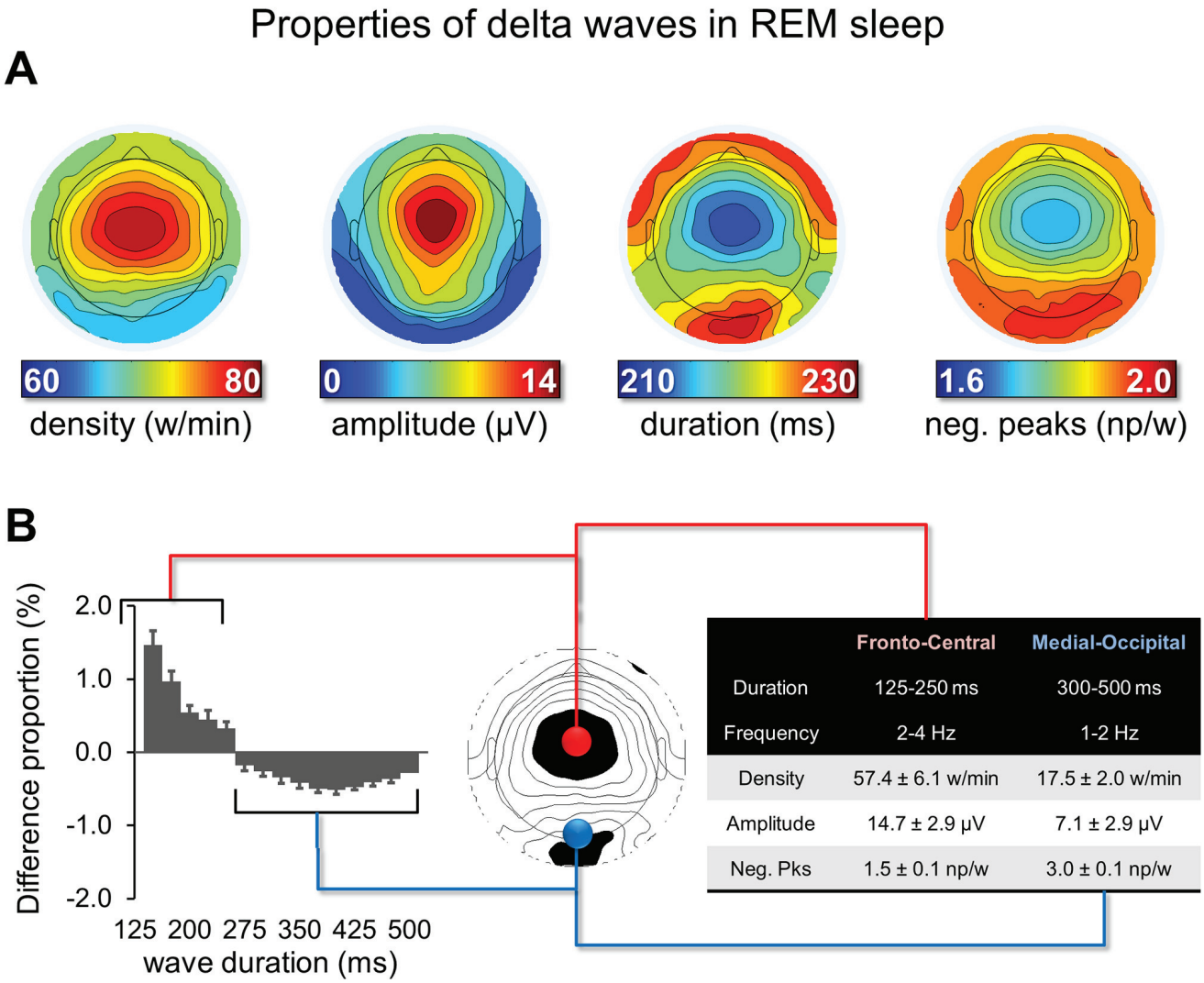

	Fronto-Central	Medial-Occipital
Duration	125-250 ms	300-500 ms
Frequency	2-4 Hz	1-2 Hz
Density	57.4 ± 6.1 w/min	17.5 ± 2.0 w/min
Amplitude	14.7 ± 2.9 μV	7.1 ± 2.9 μV
Neg. Pks	1.5 ± 0.1 np/w	3.0 ± 0.1 np/w

Temporal distribution of delta waves (bursts)

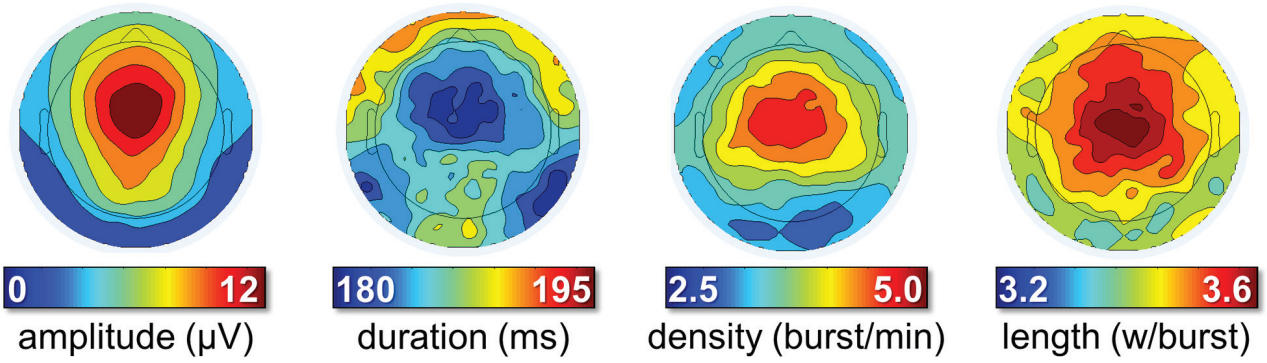

Relationship between fronto-central and medial-occipital waves

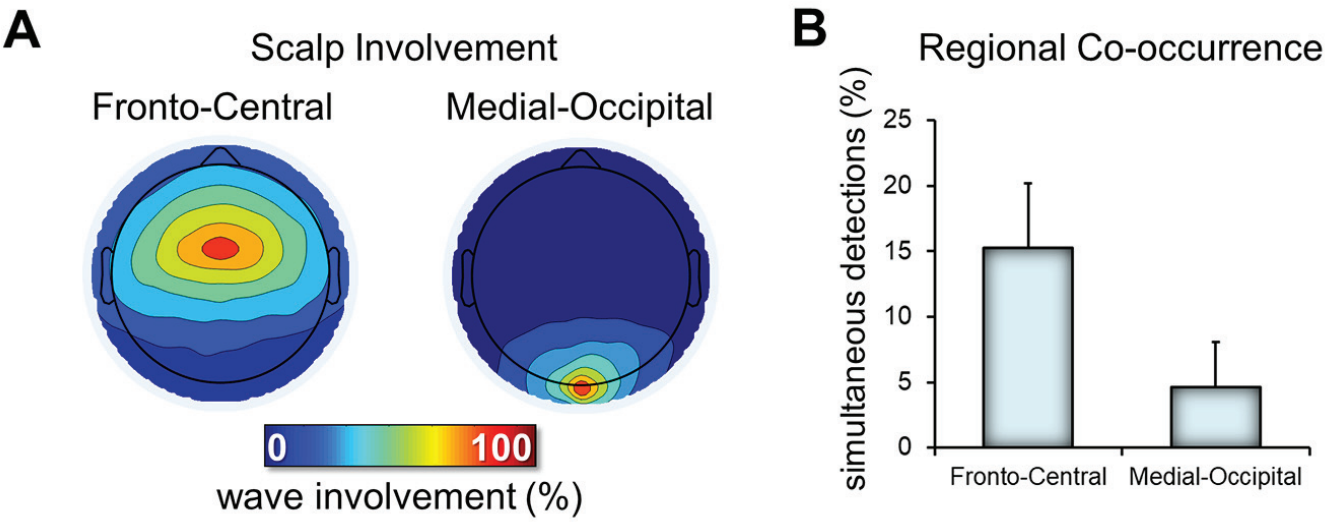

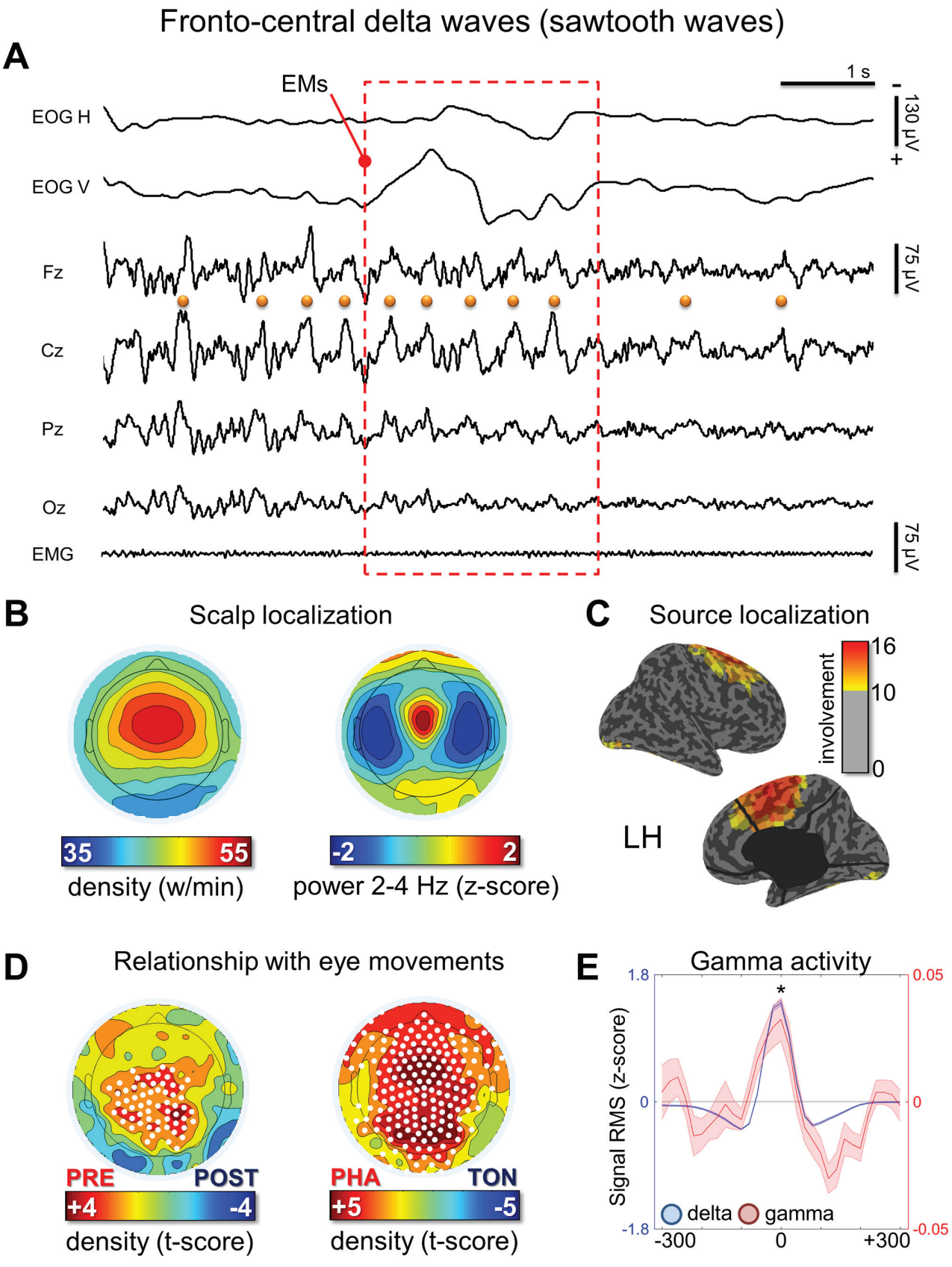

Correlation between sawtooth waves and EMs

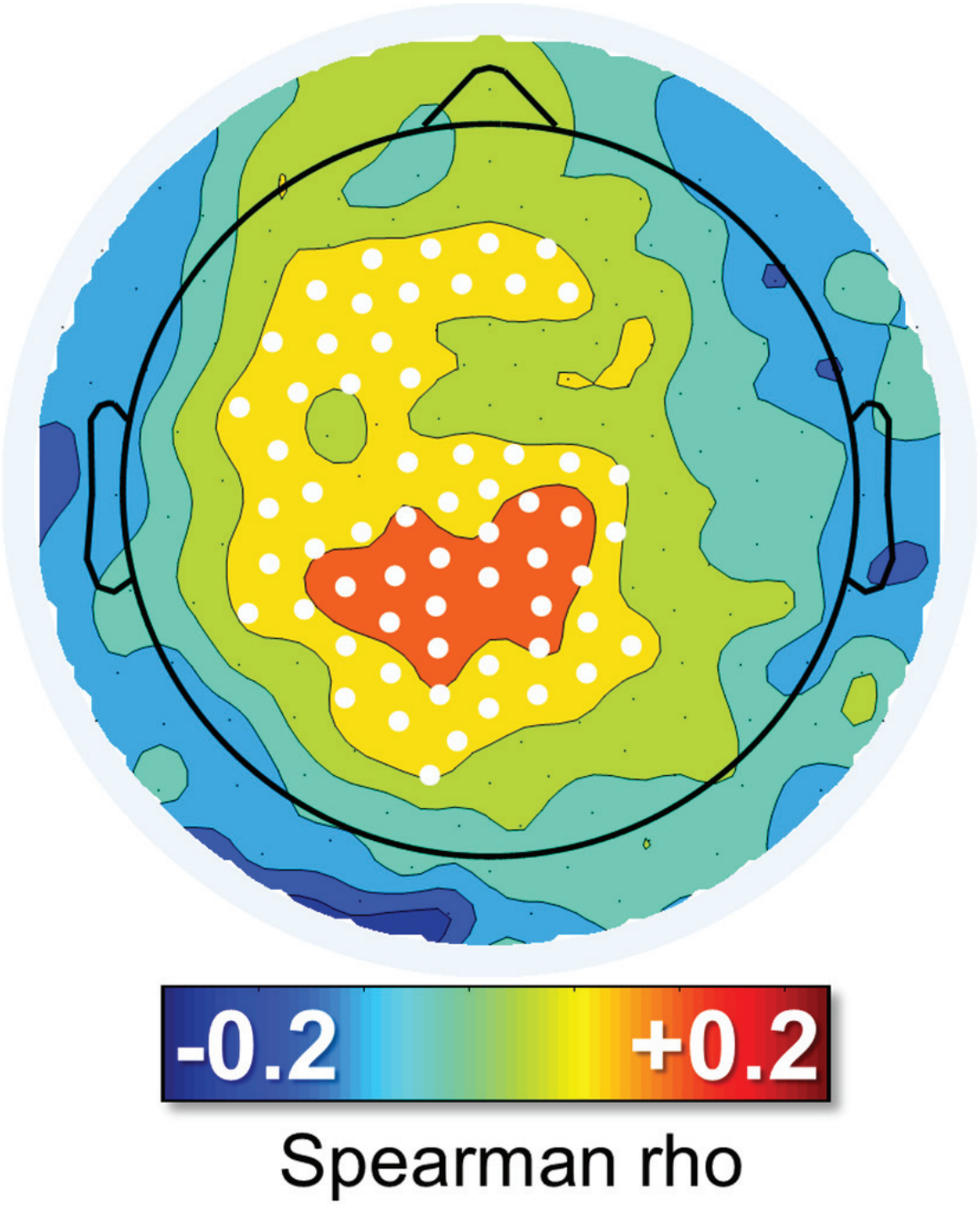

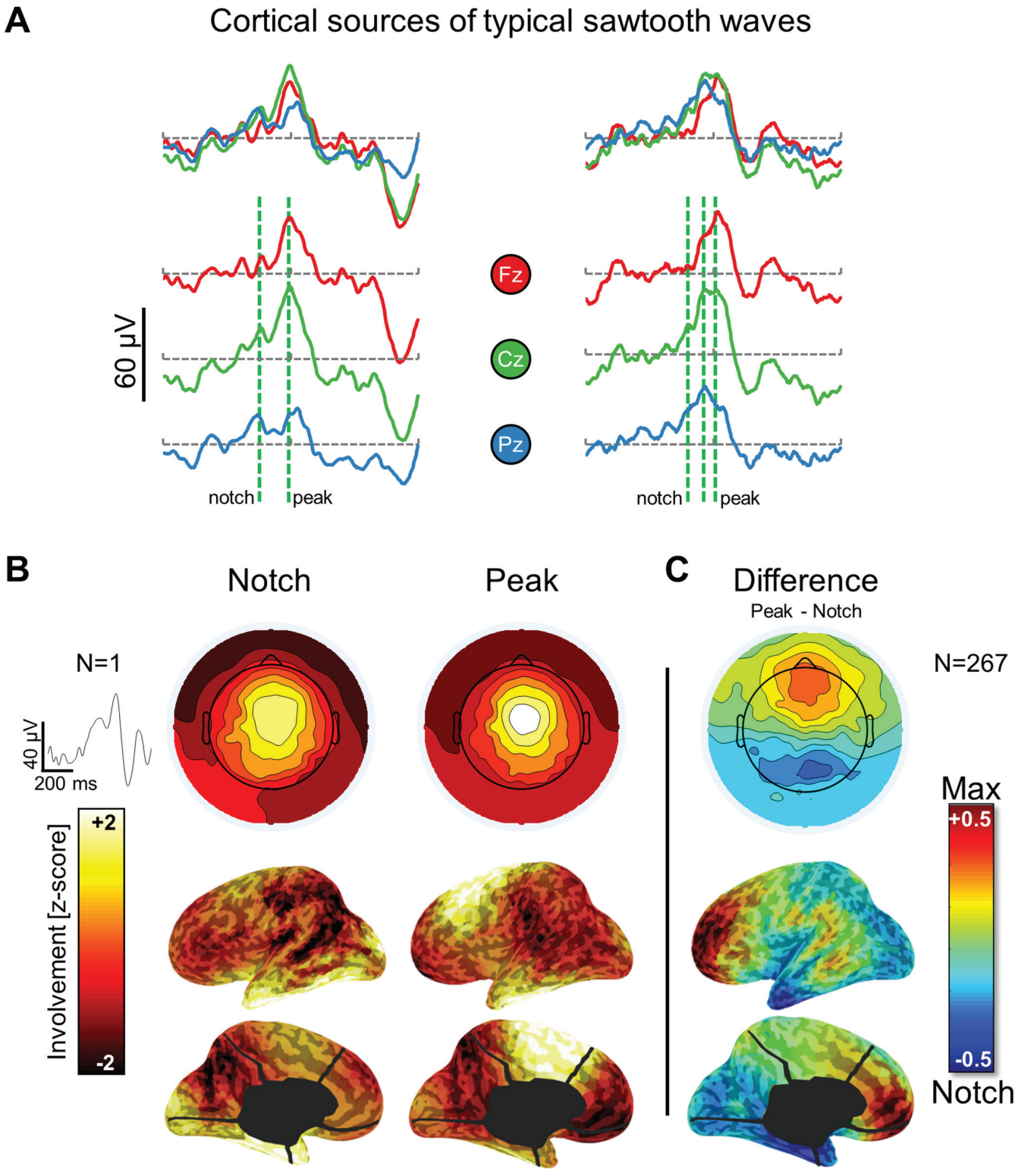

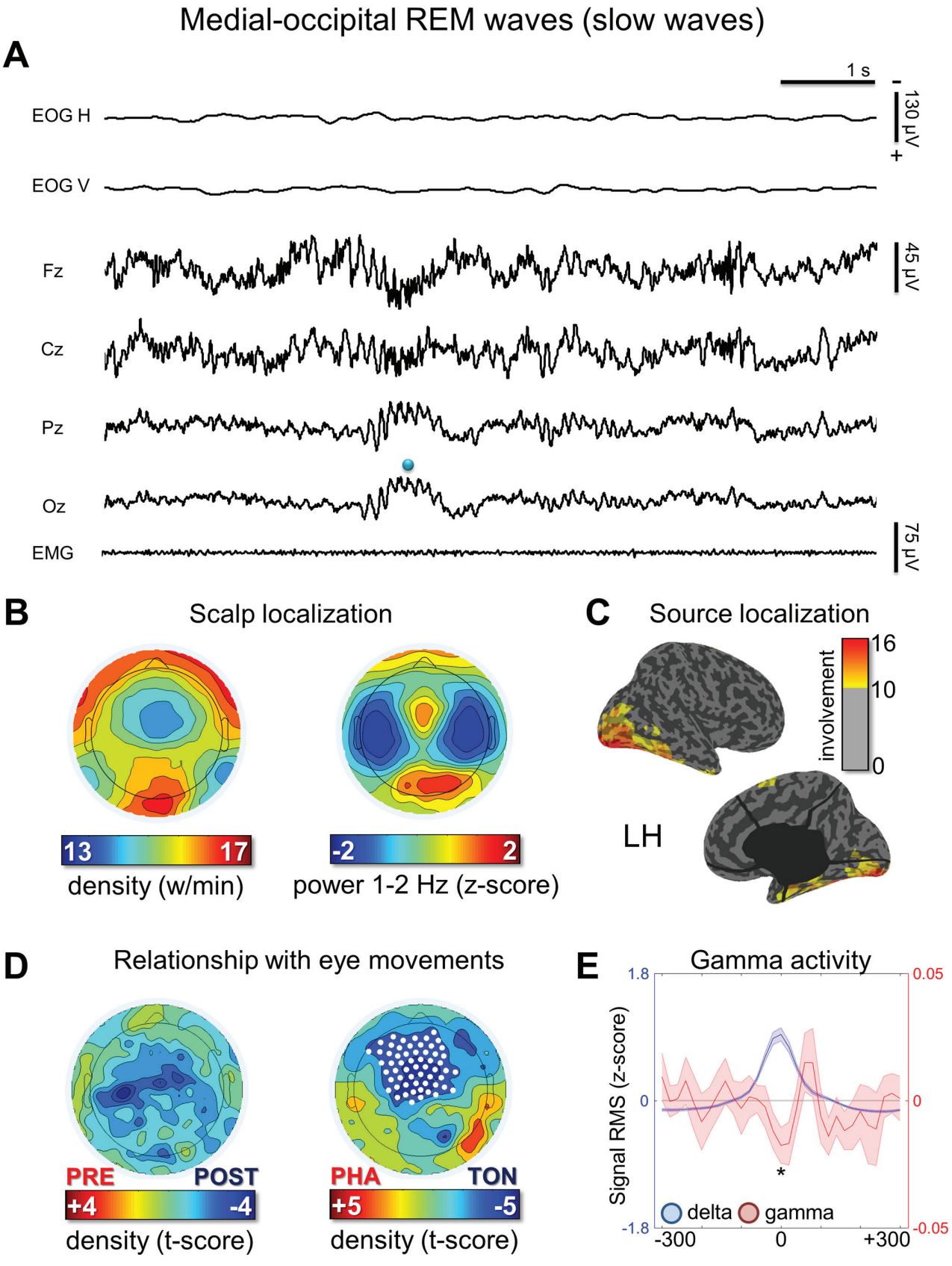

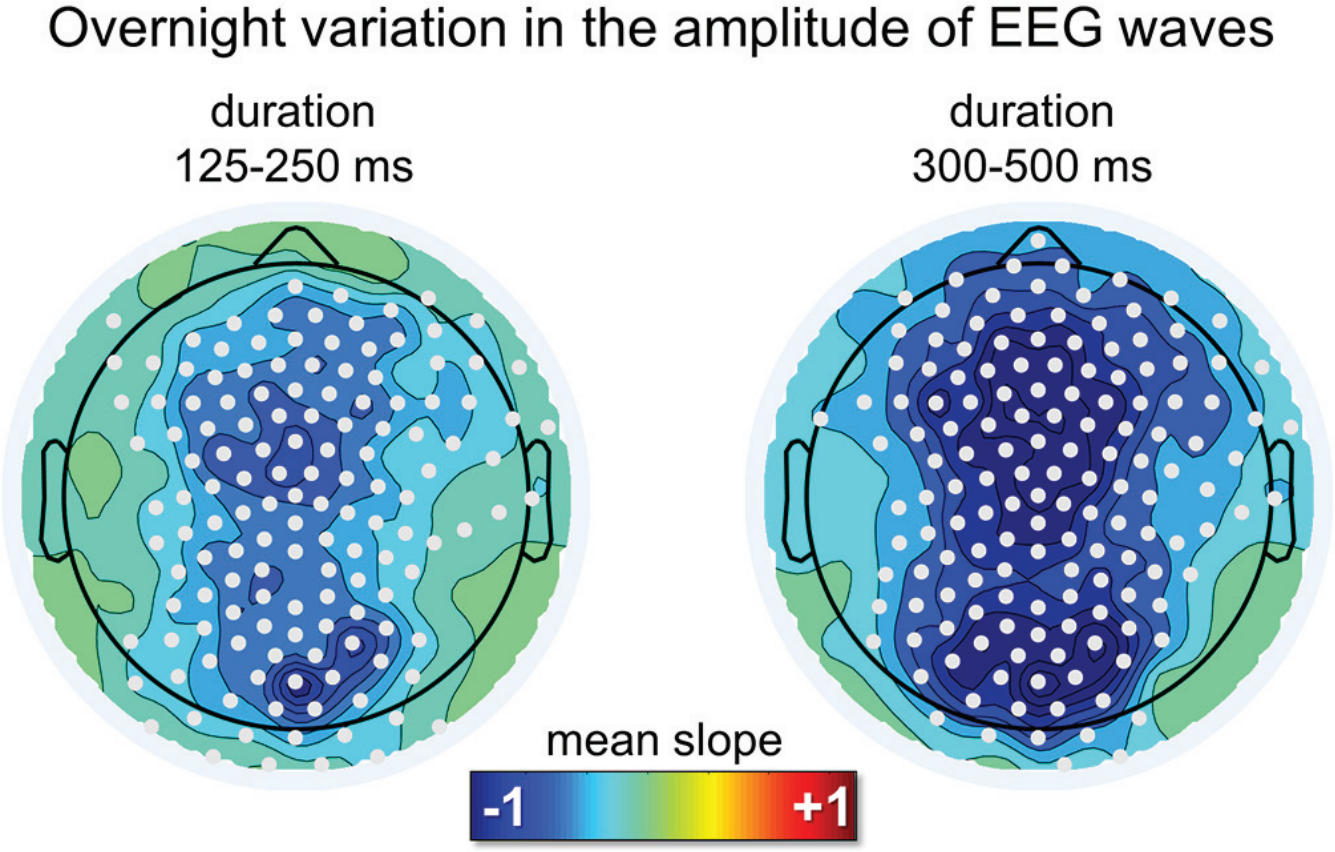

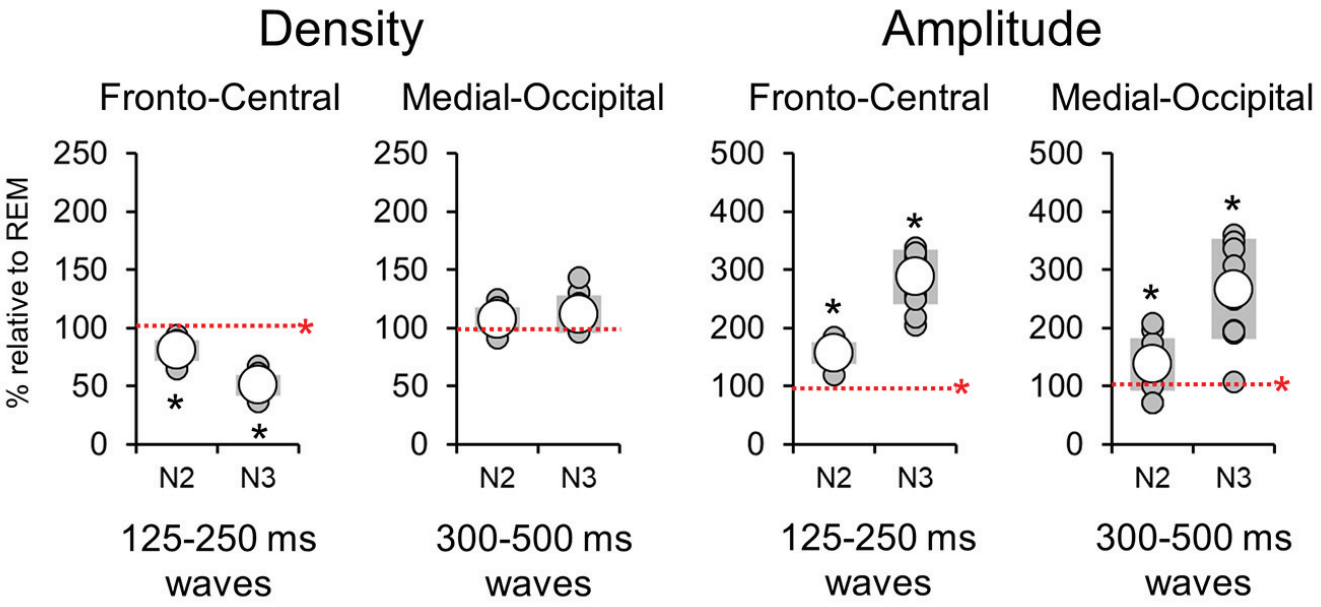

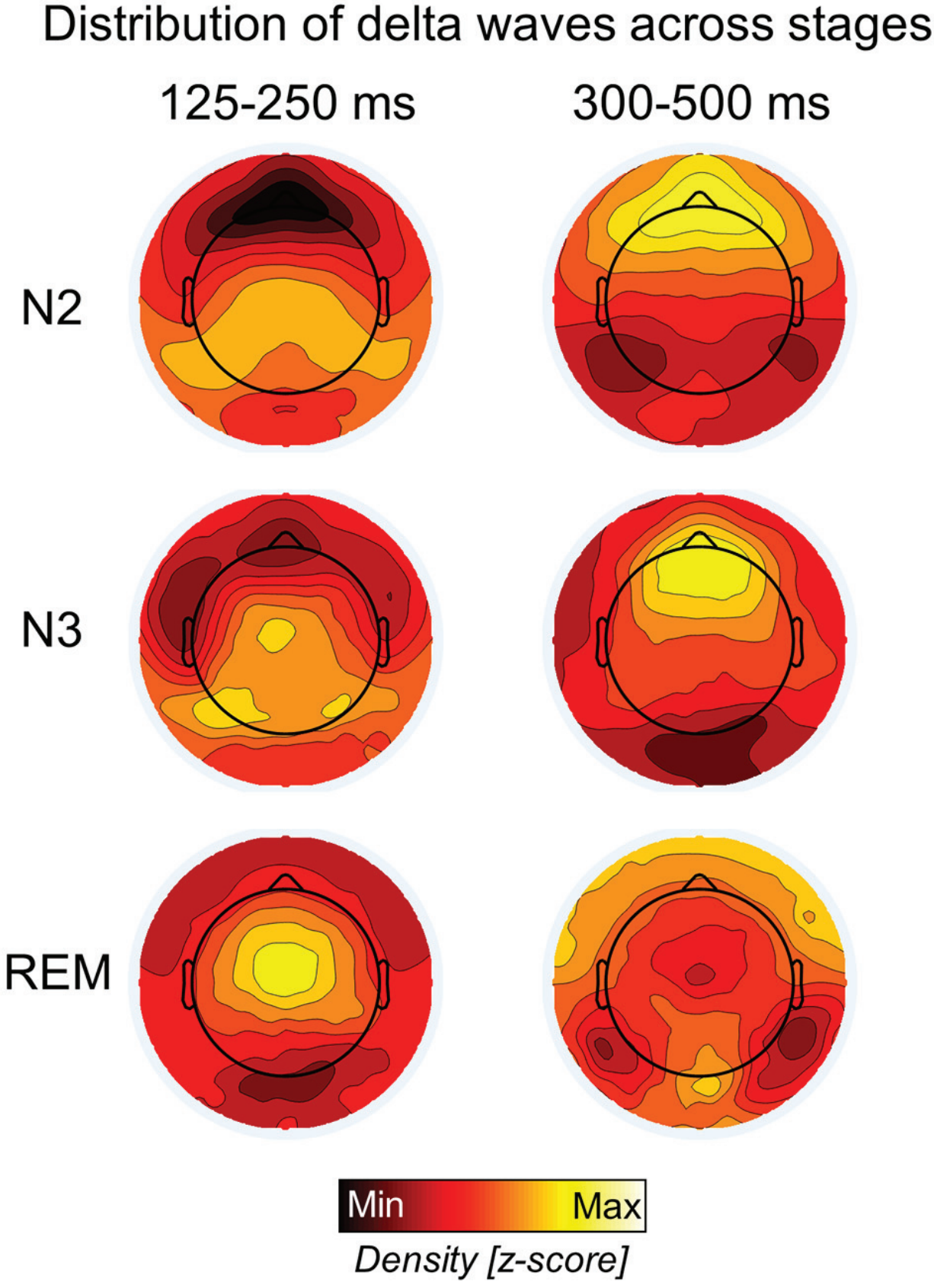

Table 1 - Sleep parameters

Parameter (N=16)	Average	SD
Total Sleep Time (min)	397.5	79.8
N1 Time (min)	21.8	15.2
N1 Proportion (%)	5.6	4.2
N2 Time (min)	209.5	52.1
N2 Proportion (%)	52.9	9.0
N3 Time (min)	78.0	29.6
N3 Proportion (%)	20.0	6.5
REM Time (min)	88.3	33.3
REM Proportion (%)	21.5	6.1
REM Latency (min)	91.5	33.5
REM Cycles (n)	4.0	1.4

Table 1. Sleep parameters (average and standard deviation) for the 16 subjects included in the study.